
Remote estimation of geologic composition using interferometric synthetic-aperture radar in California's Central Valley

Kyongsik Yun, Kyra Adams, John Reager, Zhen Liu,
Caitlyn Chavez, Michael Turmon, Thomas Lu

NASA Jet Propulsion Laboratory, California Institute of Technology

4800 Oak Grove Drive, Pasadena, CA 91109

Kyongsik.yun@jpl.nasa.gov

Abstract

1 California's Central Valley is the national agricultural center, producing 1/4 of the
2 nation's food. However, land in the Central Valley is sinking at a rapid rate (as
3 much as 20 cm per year) due to continued groundwater pumping. Land subsidence
4 has a significant impact on infrastructure resilience and groundwater
5 sustainability. In this study, we aim to identify specific regions with different
6 temporal dynamics of land displacement and find relationships with underlying
7 geological composition. Then, we aim to remotely estimate geologic composition
8 using interferometric synthetic aperture radar (InSAR)-based land deformation
9 temporal changes using machine learning techniques. We identified regions with
10 different temporal characteristics of land displacement in that some areas (e.g.,
11 Helm) with coarser grain geologic compositions exhibited potentially reversible
12 land deformation (elastic land compaction). We found a significant correlation
13 between InSAR-based land deformation and geologic composition using random
14 forest and deep neural network regression models. We also achieved significant
15 accuracy with 1/4 sparse sampling to reduce any spatial correlations among data,
16 suggesting that the model has the potential to be generalized to other regions for
17 indirect estimation of geologic composition. Our results indicate that geologic
18 composition can be estimated using InSAR-based land deformation data. In-situ
19 measurements of geologic composition can be expensive and time consuming and
20 may be impractical in some areas. The generalizability of the model sheds light
21 on high spatial resolution geologic composition estimation utilizing existing
22 measurements.

1 Introduction

24 The Central Valley aquifer system is home to 6 million residents, 250 different crops, and a \$17
25 billion per annum agricultural industry. Groundwater from the Central Valley is a valuable resource
26 that complements surface water, especially during times of drought or limited surface water
27 availability. It is a heterogeneous aquifer system with confined, semi-confined, and unconfined
28 aquifers where fresh groundwater occurs in alluvial deposits down to 3000ft [1]–[3].

29 Due to extensive agricultural activity and land use, the groundwater system in Central Valley has
30 steadily suffered groundwater loss, estimated to be around 125 million acre-feet of groundwater
31 drained between 1920-2013. This groundwater extraction has led parts of the aquifer to land
32 subsidence, as rearranging of groundwater-suspended sediment grains compacts aquifer layers.
33 Inelastic subsidence causes severe damage within the aquifer system, such as infrastructural damage
34 and loss of groundwater storage space.

35 As the groundwater is pumped, the pore space between fine-grained silts and clay decreases,
36 lowering the land surface. Compacted land cannot store as much groundwater as it used to. Some
37 land compactions are reversible, and some are not, depending on the geologic composition. The
38 types of subsidence may also change over time. Once reversible subsidence regions would
39 experience continued compaction and become irreversible regions [4]–[7]. It is important to identify
40 the type of subsidence, because we can take appropriate actions to each type of subsidence [8]. We
41 will be able to recharge groundwater for reversible or elastic regions, and strictly control
42 groundwater usage for irreversible or inelastic regions.

43 In-situ geologic composition quantification is important in managing groundwater and
44 preventing/recovering land subsidence, yet costly and labor intensive. Moreover, understanding
45 geologic composition is essential for hydrological models for future predictive models of land
46 subsidence and groundwater levels, especially in regions where extensive geologic data are not
47 available. In this study, we aim to indirectly quantify geologic composition based on temporally
48 changing remote land deformation information using InSAR.

49 **2 Methods**

50 **2.0 InSAR data processing**

51 We processed Sentinel-1 (S-1) satellite data of track 42 and 144 from 2015/03/01 to 2020/08/31 and
52 2014/11/08-2019/01/22, respectively to estimate ground movement associated with groundwater
53 withdrawal/recharging in the Central Valley, California. The two tracks cover most of the central
54 and southern Central Valley including San Joaquin Valley and Tulare Basin. The S-1 satellite
55 constellation has been acquiring interferometric wide-swath mode data over the Central Valley with
56 a regular interval of 12 days and a revisit time as short as 6 days using terrain observation by
57 progressive scan (TOPS) technique. We use the JPL/Caltech ISCE software to generate the S-1
58 interferometry and limit our interferometric pairs to the ones with temporal baseline no more than
59 24 days. This mitigates temporal decorrelation. We then use a sentinel-1 stack processor to co-
60 register all SAR single look complex (SLC) images to the reference geometry and employ the
61 enhanced spectral diversity technique to estimate azimuth misregistration between SLC images in a
62 stack sense. Each interferogram is corrected for topographic phase and then unwrapped and
63 geocoded using SRTM DEM model. After generating hundreds of unwrapped interferograms for
64 each track, we use a variant of the Small Baseline Subset InSAR time series inversion approach to
65 solve for line-of-sight (LOS) displacement time series and mean velocity. The approach also
66 estimates the DEM error and uses spatiotemporal filtering to suppress high-frequency troposphere
67 noise. For more details about the InSAR processing and time series analysis, please refer to Liu et
68 al. (2019) [9]. The cumulative LOS displacements at each image date are outputted to a GMT grid,
69 which is resampled to a ground posting of ~2km x 2km.

70 **2.1 Geologic composition**

71 The data for geologic composition was obtained from the geotexture model published as part of the
72 USGS Central Valley Hydrologic Model (CVHM). The geotexture model was created based on
73 lithologic data from 8,500 borehole logs, with depth reaching down to 3000ft from land surface.
74 The lithologic data was classified in binary bins of fine-grained or coarse-grained. This was based
75 on the original description in the log, with coarse-grained sediments encompassing sand, gravel,
76 pebbles, and boulders and fine-grained sediments encompassing clay, lime, loam, mud, or silt. Then
77 the percentage of fine-grained and coarse-grained sediments were calculated in 50ft segments. The
78 texture model arrays are organized in the same dimensions as the groundwater flow model, with 1-
79 mi by 1-mi grid cells and 10 modeling layers based on horizontal geologic characteristics. Roughly
80 20,000 model cells are active within the Central Valley. Readers are pointed to Faunt (2009) [10]
81 for more details on the geotexture model.

82 Coarse grain percent of each model layer from 1 to 10 in northern and southern Central Valley
83 regions was used as the prediction target (Supplementary Figure 1). Coarse-grained soil is defined
84 as containing no more than 50% fine grains (i.e., silt and clay, or particles smaller than 0.075 mm).

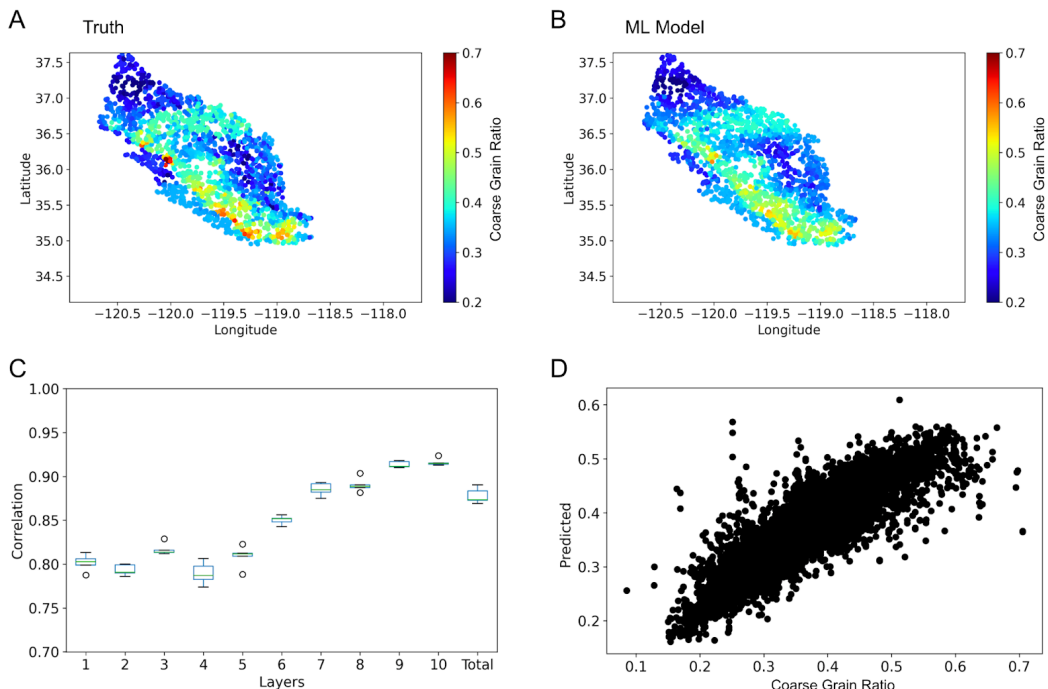
85 **2.2 Data interpolation**

86 We first integrated multimodal data including InSAR, groundwater, precipitation, and geologic
 87 composition by interpolating data with the same spatial and temporal resolutions (every 2 weeks on
 88 a 2kmX2km grid) (Supplementary Figures 2 & 3). We then identified regions with different temporal
 89 dynamics of land displacement, groundwater depth, precipitation, and geologic composition
 90 (Supplementary Figure 4). Some areas (e.g., Helm) with coarser grain geologic compositions
 91 exhibited potentially reversible land transformations (elastic land compaction).

92 2.3 Geologic estimation models

93 We used long short-term memory (LSTM) as a recurrent network component. Conventional
 94 recurrent neural networks still have significant practical problems caused by exponential decay of
 95 gradient descent, which hinders learning of long-term relationships between time points. LSTM is
 96 a special type of recurrent neural network that can learn long-term dependencies through selective
 97 memory consolidation [11]. We used 3 convolutional input layers, 6 recurrent layers, 1 fully
 98 connected layer, and 1 softmax layer [12], [13]. Model training aims to minimize the error function
 99 E, the mean squared error (MSE) that quantifies the difference between the estimated (neural
 100 network outputs) and the true 10-layer geologic compositions (ground truth in-situ data). Input data
 101 include InSAR subsidence data, covering 8818 different locations, and 132 biweekly time points (5
 102 years). Here, the coarse grain percent of 10 layers was estimated.

103



104
 105 Figure 1. Geologic composition prediction using InSAR land deformation data. (A) Ground truth
 106 coarse grain ratio of the entire layer and (B) estimated coarse grain ratio. (C) Correlation between
 107 model output and ground truth at different layers of geologic composition. (D) Scatter plot
 108 between the ground truth and estimated geologic composition of the entire layer ($R=0.88$).

109 3 Results

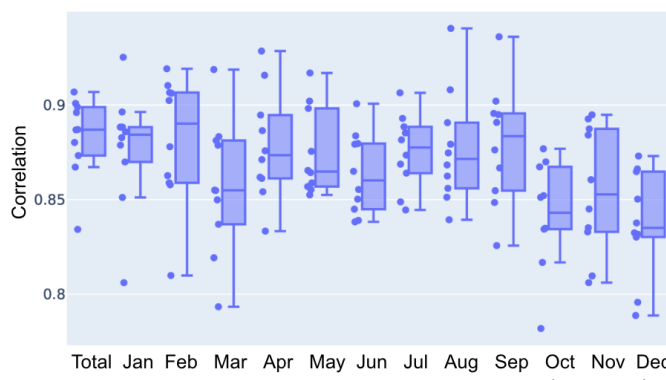
110 We found that the InSAR remote sensing data had predictive power for geologic composition using
 111 deep neural networks (correlation coefficient $R=0.88$) (Figure 1). A decision tree ($R=0.65$) and
 112 random forest model ($R=0.85$) was tested as baseline. We also achieved significant accuracy with
 113 only 40% of the training data ($R=0.80$), suggesting that the model can be generalized to other regions
 114 for indirect estimation of geologic composition. We performed an estimation with distant data
 115 sampling (minimum distance between samples was 10km) to reduce the impact of spatial correlation
 116 of adjacent data points, and we found a slightly degraded performance ($R=0.83$) (Supplementary

117 Figure 5).

118 4 Discussion

119 In this study, we showed that geological composition can be estimated remotely using InSAR land
120 deformation data. In-situ measurements of geological composition are critical to understanding
121 hydrology and monitoring groundwater availability. However, in-situ measurements are expensive
122 and time consuming. If geologic composition can be measured remotely using this model, high
123 spatial resolution geologic composition can be quickly quantified only with InSAR satellites without
124 in-situ measurements. The next step is to apply this model to other regions, including US High Plains
125 and North China Plains, to evaluate its generalizability [14].

126 As a further analysis to determine which time of year contributed the most to the estimation of
127 geologic composition, we performed a leave-one-month-out 10-fold cross-validation performance
128 test (Figure 2). When we excluded the October and December data from the estimation model, we
129 found a significant decline in correlation, indicating that this month contributed the most to
130 estimating the geological composition. Most of the precipitation occurs in late autumn and winter,
131 and precipitation has influenced time-series changes in InSAR land deformation, indirectly
132 indicating the inner geological composition of the Central Valley.



134
135 Figure 2. Leave-one-month-out 10-fold cross-validation performance test. Correlation degradation
136 was computed as each month was excluded from the input parameters of the model. October
137 ($p=0.00175$) and December ($p=0.000654$) showed significant degradation compared to total data
138 correlation. The statistical significance cut-off is at $p=0.004$ considering Bonferroni multiple
139 comparisons (0.05/12 comparisons=0.004).

140

141 One caveat of this study is the lack of ground truth geologic composition data for independent model
142 validation. In-situ geologic composition data from other regions (e.g., US High Plains, North China
143 Plains) will be required for further testing. At the same time, the lack of geologic composition data
144 points to the advantage of a significant potential applicability of this model. Our suggested model
145 can be applicable to future missions such as NISAR and NASA's Decadal Survey Designated
146 Observables like Mass Change (MC) and Surface Deformation and Change (SDC) as an indirect
147 geologic composition product [15].

148 Acknowledgments

149 The research was carried out at the Jet Propulsion Laboratory, California Institute of Technology,
150 under a contract with the National Aeronautics and Space Administration.

151 References

- 152 [1] C. D. Farrar and G. L. Bertoldi, "Region 4, central valley and pacific coast ranges," 1988.
- 153 [2] R. W. Page, *Geology of the fresh ground-water basin of the Central Valley, California: With texture maps and sections*. US Government Printing Office, 1986.

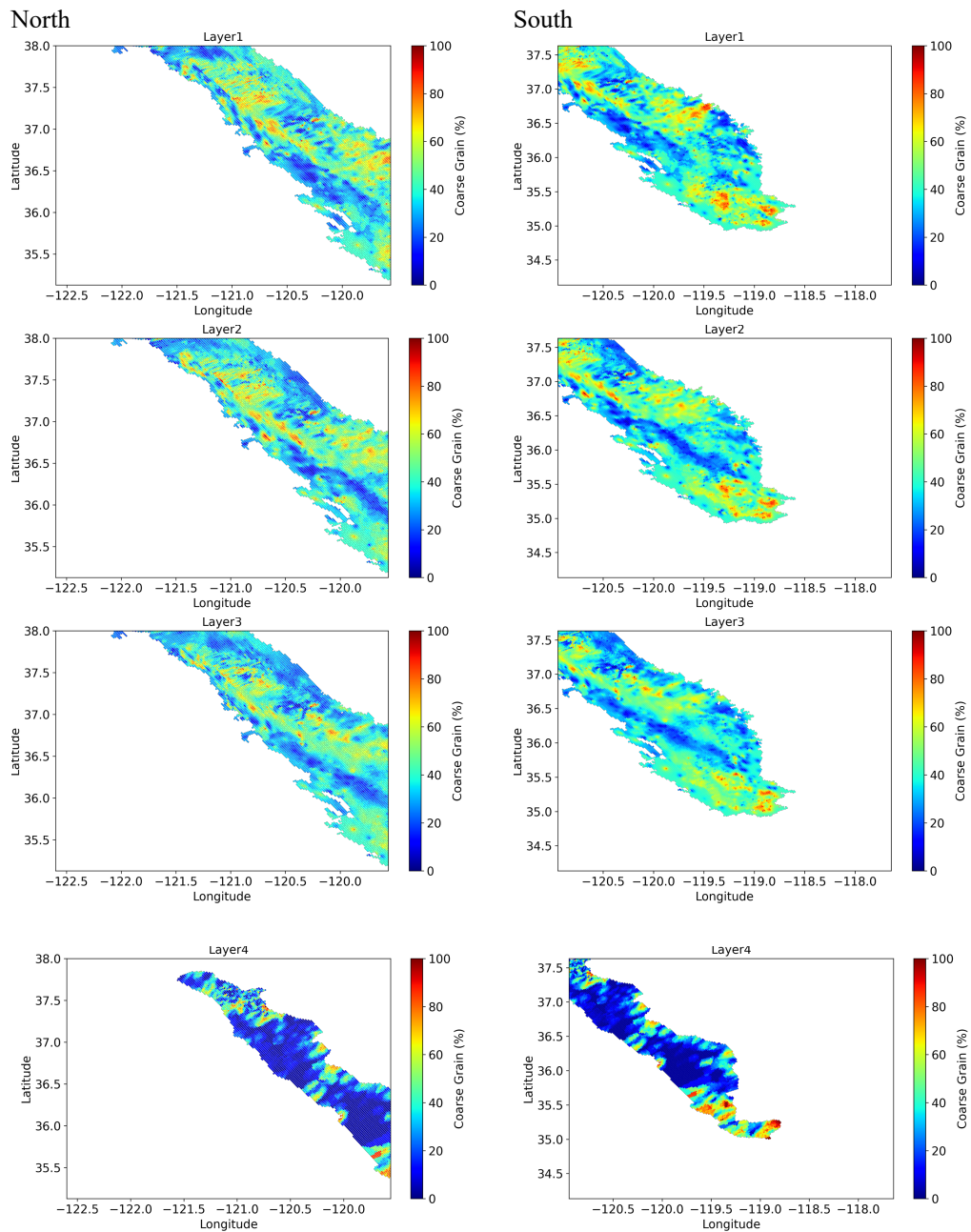
- 155 [3] A. K. Williamson, D. E. Pradic, and L. A. Swain, *Ground-water flow in the Central Valley, California*. US Government Printing Office, 1989.
- 156 [4] S. M. J. Mirzadeh *et al.*, “Characterization of Irreversible Land Subsidence in the Yazd-Ardakan Plain, Iran From 2003 to 2020 InSAR Time Series,” *Journal of Geophysical Research: Solid Earth*, vol. 126, no. 11, p. e2021JB022258, 2021.
- 157 [5] D. L. Galloway, D. R. Jones, and S. E. Ingebritsen, *Land subsidence in the United States*, vol. 1182. US Geological Survey, 1999.
- 158 [6] R. Maliva and T. Missimer, “Compaction and land subsidence,” in *Arid Lands Water Evaluation and Management*, Springer, 2012, pp. 343–363.
- 159 [7] T. G. Farr and Z. Liu, “Monitoring subsidence associated with groundwater dynamics in the Central Valley of California using interferometric radar,” *Remote Sensing of the Terrestrial Water Cycle*, vol. 206, p. 397, 2014.
- 160 [8] B. R. Scanlon *et al.*, “Groundwater depletion and sustainability of irrigation in the US High Plains and Central Valley,” *Proceedings of the National Academy of Sciences*, vol. 109, no. 24, pp. 9320–9325, 2012, doi: 10.1073/pnas.1200311109.
- 161 [9] Z. Liu, P.-W. Liu, E. Massoud, T. G. Farr, P. Lundgren, and J. S. Famiglietti, “Monitoring Groundwater Change in California’s Central Valley Using Sentinel-1 and GRACE Observations,” *Geosciences*, vol. 9, no. 10, p. 436, 2019.
- 162 [10] C. C. Faunt, “Geological Survey (US)(Eds.): Groundwater availability of the Central Valley Aquifer, California,” *US Geological Survey professional paper*, US Geological Survey, Reston, VA, 2009.
- 163 [11] S. Hochreiter, Y. Bengio, P. Frasconi, and J. Schmidhuber, “A field guide to dynamical recurrent neural networks,” in *chapter Gradient Flow in Recurrent Nets: The Difficulty of Learning Long-Term Dependencies*, Wiley-IEEE Press, 2001, pp. 237–243.
- 164 [12] D. Amodei *et al.*, “Deep speech 2: End-to-end speech recognition in english and mandarin,” in *International conference on machine learning*, 2016, pp. 173–182.
- 165 [13] K. Yun, T. Lu, and A. Huyen, “Transforming unstructured voice and text data into insight for paramedic emergency service using recurrent and convolutional neural networks,” in *Pattern Recognition and Tracking XXXI*, 2020, vol. 11400, p. 1140006.
- 166 [14] G. Herrera-García *et al.*, “Mapping the global threat of land subsidence,” *Science*, vol. 371, no. 6524, pp. 34–36, Jan. 2021, doi: 10.1126/science.abb8549.
- 167 [15] S. S. Board and N. R. Council, *Earth science and applications from space: a midterm assessment of NASA’s implementation of the decadal survey*. National Academies Press, 2012.

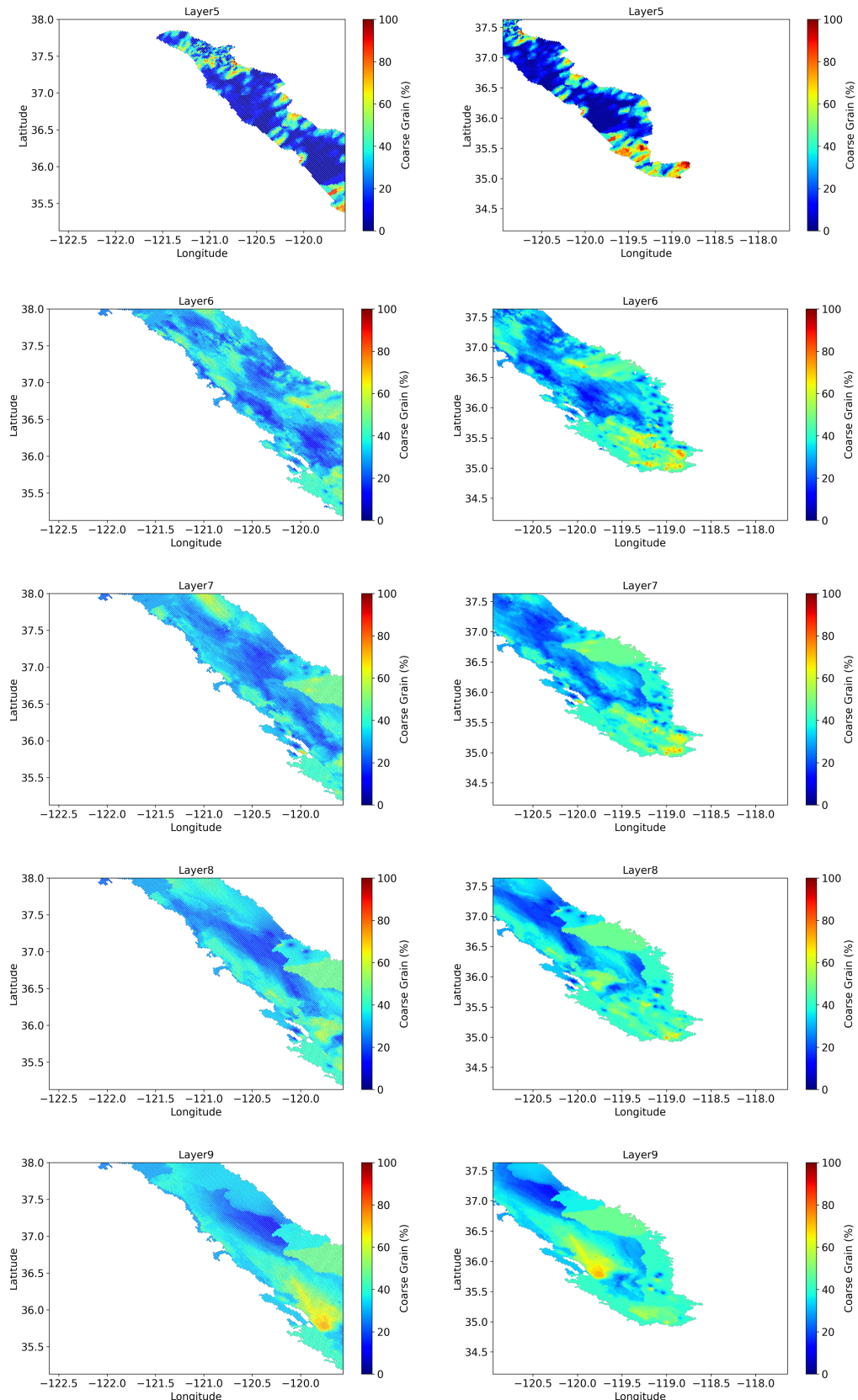
189

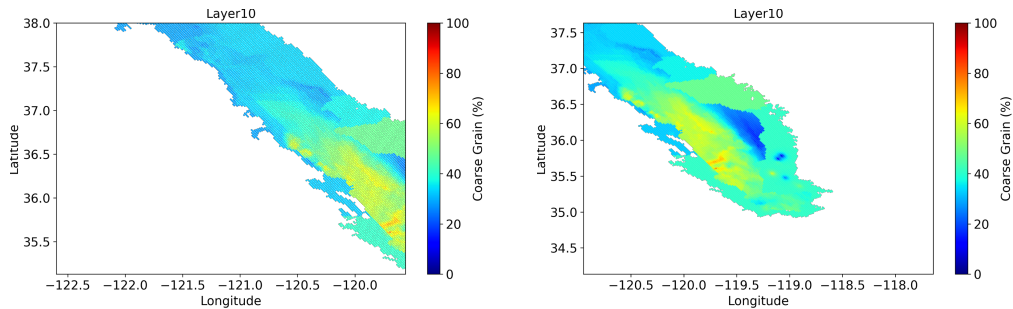
190 **Supplementary Information**

191 Supplementary Figure 1. Coarse Grain (%) of each layer from 1 to 10 in northern and southern
192 Central Valley regions.

193

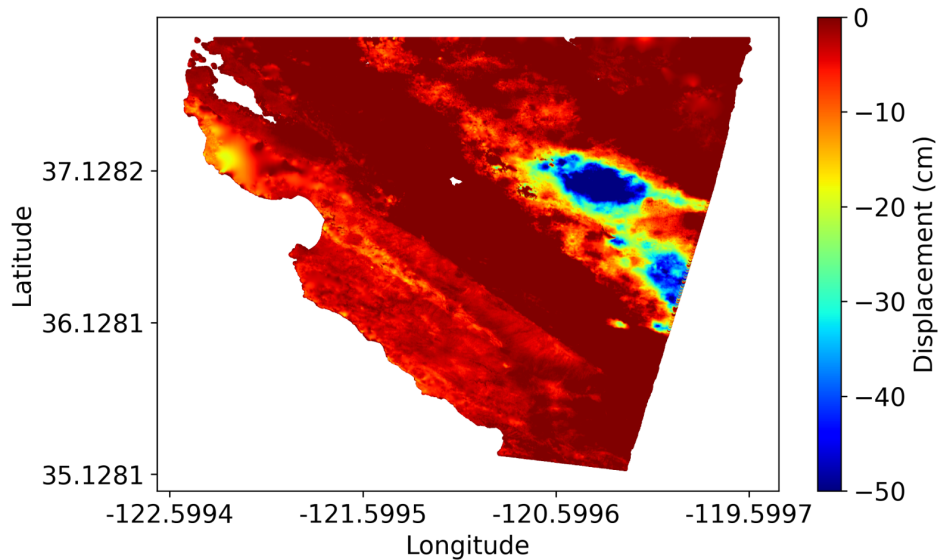






194

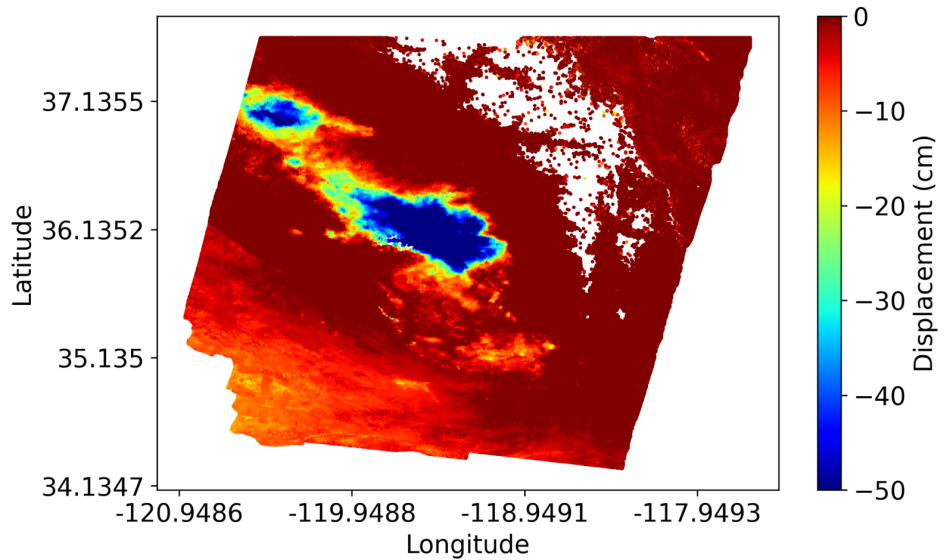
195 Supplementary Figure 2. Northern Central Valley InSAR land displacement (March 1, 2015 ~
196 August 31, 2020)



197

198

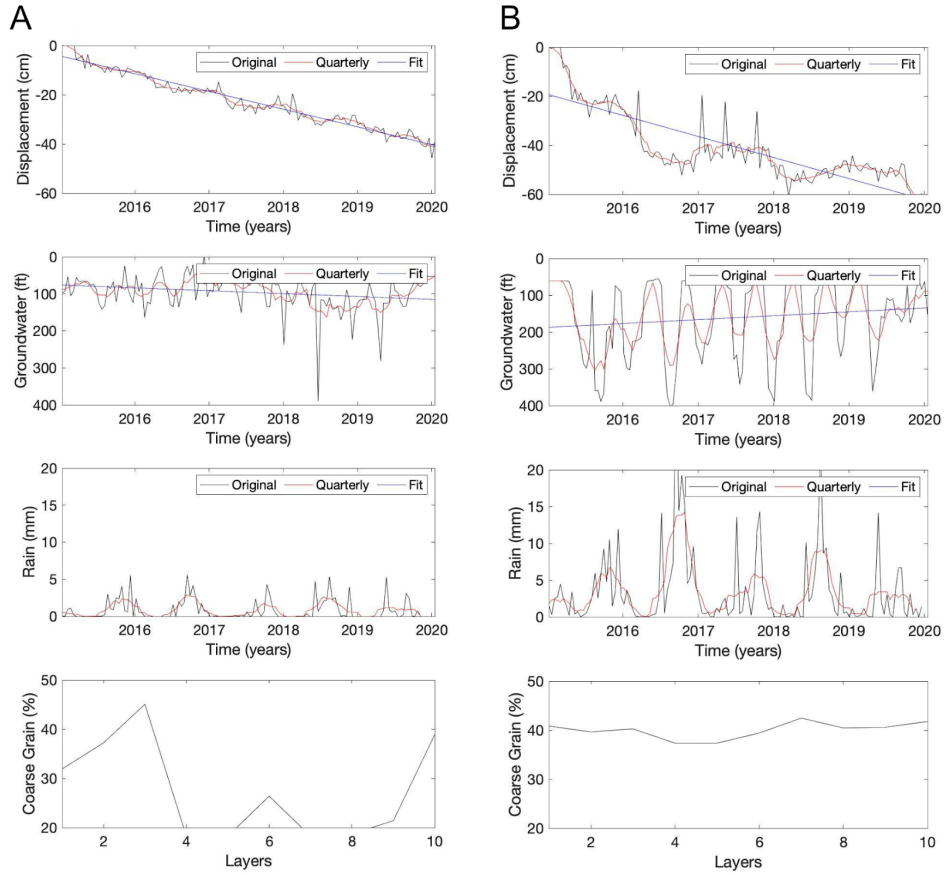
199 Supplementary Figure 3. Southern Central Valley InSAR land displacement (November 8, 2014 ~
200 January 22, 2019)



201

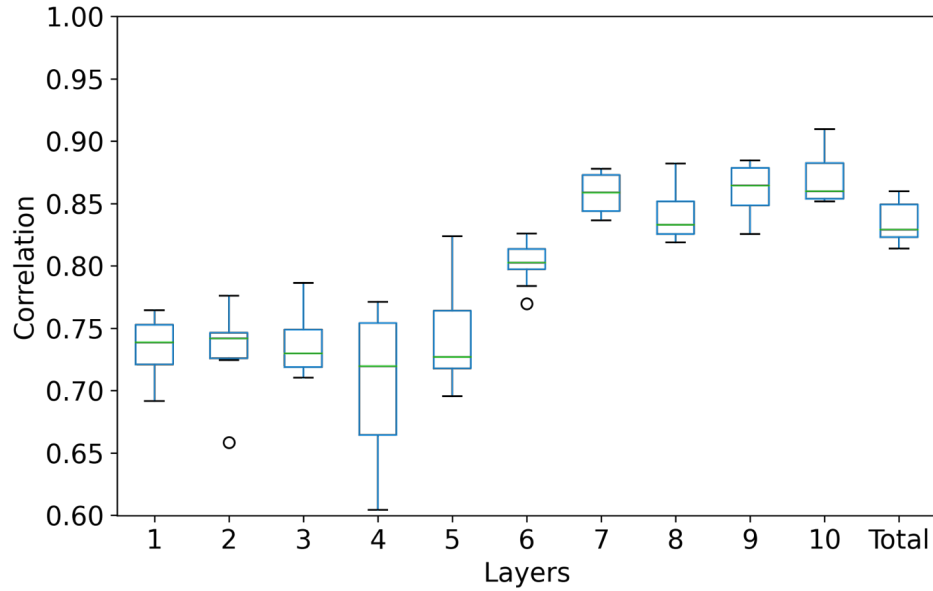
202

203 Supplementary Figure 4. Two representative regions of the Central Valley with significant
 204 subsidence with different characteristics. (A) Chowchilla has been shown to maintain monotonically
 205 decreasing land displacements, less fluctuating groundwater depth, relatively low precipitation, and
 206 high fine-grain ratio across the middle soil layers (Displacement = -22.47 ± 10.66 , Groundwater (ft)
 207 = 95.53 ± 27.69 , Rain (mm) = 0.84 ± 0.80 , Coarse Grain (%) = 27.44 ± 10.13). (B) Helm, on the
 208 other hand, exhibited fluctuating land displacements, relatively large seasonal changes in
 209 groundwater depth, high precipitation, and a higher overall coarse-grain ratio across all soil layers
 210 (Displacement = -40.95 ± 14.49 , Groundwater (ft) = 160.52 ± 65.82 , Rain (mm) = 3.48 ± 3.15 ,
 211 Coarse Grain (%) = 40.01 ± 1.67).



212
 213
 214
 215

216 Supplementary Figure 5. Geologic composition prediction with distant data sampling (minimum
217 distance between samples was 10km) using InSAR land deformation data. Distant data sampling
218 was performed to reduce the impact of spatial correlation of adjacent data points. Total prediction
219 performance dropped from 0.88 to 0.83, but remained largely unchanged.



220
221